Published in final edited form as:
Hear Res. 2010 September 1; 268(1-2): 2–11. doi:10.1016/j.heares.2010.04.014.

Murine Intracochlear Drug Delivery: Reducing Concentration Gradients within the Cochlea

David A. Borkholder[1,2,3], **Xiaoxia Zhu**[2,5], **Brad T. Hyatt**[2], **Alfredo S. Archilla**[2], **William J. Livingston III**[2], and **Robert D. Frisina**[2,3,4,5]

[1]Department of Electrical and Microelectronic Engineering, Rochester Institute of Technology, Rochester, NY 14623, USA

[2]Department of Otolaryngology, University of Rochester Medical School, Rochester, NY, 14642, USA.

[3]Department of Biomedical Engineering, University of Rochester Medical School, Rochester, NY, 14642, USA.

[4]Department Neurobiology & Anatomy, University of Rochester Medical School, Rochester, NY, 14642, USA.

[5]International Center for Hearing & Speech Research, National Technical Institute for the Deaf, Rochester Institute of Technology, Rochester, NY, 14623, USA

Abstract

Direct delivery of compounds to the mammalian inner ear is most commonly achieved by absorption or direct injection through the round window membrane (RWM), or infusion through a basal turn cochleostomy. These methods provide direct access to cochlear structures, but with a strong basal-to-apical concentration gradient consistent with a diffusion-driven distribution. This gradient limits the efficacy of therapeutic approaches for apical structures, and puts constraints on practical therapeutic dose ranges. A surgical approach involving both a basal turn cochleostomy and a posterior semicircular canal canalostomy provides opportunities for facilitated perfusion of cochlear structures to reduce concentration gradients. Infusion of fixed volumes of artificial perilymph (AP) and sodium salicylate were used to evaluate two surgical approaches in the mouse: cochleostomy-only (CO), or cochleostomy-plus-canalostomy (C+C). Cochlear function was evaluated via closed-system distortion product otoacoustic emissions (DPOAE) threshold level measurements from 8-49 kHz. AP infusion confirmed no surgical impact to auditory function, while shifts in DPOAE thresholds were measured during infusion of salicylate and AP (washout). Frequency dependent shifts were compared for the CO and C+C approaches. Computer simulations modeling diffusion, volume flow, interscala transport, and clearance mechanisms provided estimates of drug concentration as a function of cochlear position. Simulated concentration profiles were compared to frequency-dependent shifts in measured auditory responses using a cochlear tonotopic map. The impact of flow rate on frequency dependent DPOAE threshold shifts was also evaluated for both surgical approaches. Both the C+C approach and a flow rate increase were found to provide enhanced response for lower frequencies, with evidence suggesting the C+C approach reduces concentration gradients within the cochlea.

Corresponding Author: David A. Borkholder Rochester Institute of Technology 79 Lomb Memorial Drive Rochester, NY 14623 585-475-6067 585-475-5845 (fax) david.borkholder@rit.edu.

Keywords

mouse; drug delivery; infusion; concentration gradient; cochlea; inner ear; salicylate

Introduction

Delivery of therapeutic agents to the inner ear via absorption through the RWM has been effective in clinical treatment of tinnitus, sudden sensorineural hearing loss, and Meniere's disease (e.g., Borkholder, 2008). While effective for acute treatment of these auditory and vestibular disorders, direct quantitative measures of drug distribution within the cochlea during delivery to the RWM niche demonstrate a significant apical-basal concentration gradient in scala tympani (Plontke et al., 2008). Frequency dependent physiological responses to agents directly infused into the basal turn of scala tympani suggest similar gradients exist for direct infusion approaches (Chen et al., 2006). This gradient will impact treatment efficacy for pharmaceuticals with a narrow therapeutic window, or molecular therapies involving protection or regeneration in apical cochlear structures. Advanced therapies which address the biological basis of auditory and vestibular dysfunction will require understanding and control of concentration gradients associated with different inner ear drug delivery protocols. Animal studies coupled with computer models of the cochlea provide opportunities to test different delivery methodologies and explore potential clearance rates and modes of interscalar exchange which impact cochlear concentration gradients.

Isolation of delivered agents to the treated cochlea will become increasingly important as more toxic substances (e.g., viral vectors for gene delivery) are used to treat auditory and vestibular dysfunction. Studies involving slow infusions or bolus injections into scala tympani often report impact to the contralateral ear. Roehm and colleagues (2007) observed gentamicin transfer to the contralateral ear following middle ear perfusions, with evidence implicating the cochlear aqueduct. Stöver and co-workers (2000) examined this in detail with virus inoculation in the bloodstream, CSF, and scala tympani, identifying the cochlear aqueduct as the most likely route of virus spread to the contralateral cochlea. Protocols involving continuous perfusion into scala tympani will result in expulsion of fluid through the cochlear aqueduct unless a fluidic exit route is provided within the cochlea, or a zero net volume delivery approach is utilized as described by Chen et al. (2005).

The issues of diffusion limited access to apical cochlear structures, and isolation limited by efflux through a patent cochlear aqueduct could potentially be mitigated by *directed perfusion* through the cochlea. A basal turn scala tympani infusion (cochleostomy) coupled with an exit hole in the posterior semicircular canal (canalostomy) could create a preferential perfusion flow pattern from base to apex in scala tympani, through the helicotrema, from apex to base in scala vestibuli. The flow will depend on relative fluidic resistances of this path with that of interscalar transport and the cochlear aqueduct. This contrasts with infusion at the basal turn of scala tympani with no exit hole where presumably all excess fluid is pushed through the cochlear aqueduct into the cranial subarachnoid space with diffusion as the dominant mechanism for carrying pharmaceutical agents to the apical turns. Directed perfusion of the cochlea offers potential for reduced concentration gradients, and improved isolation of drugs / genes to target tissue.

Materials and Methods

Infusion of fixed volumes of artificial perilymph (AP) and 10mM sodium salicylate (SAL) in AP were used to evaluate the efficiency of two surgical approaches for modulating cochlear function in the mouse model system. The cochleostomy infusion approach was similar to that

described by Chen and colleagues (2006) while the directed perfusion was a combination of this approach and the posterior semicircular canal canalostomy described by Kawamoto and co-workers (2001) and Nakagawa and co-workers (2003). The canalostomy was chosen over a second cochleostomy in scala vestibuli since it provides the least difficult surgical access. Cochlear function was evaluated via DPOAE thresholds, allowing an indirect physiological estimation of drug distribution within the cochlea. While potential non-uniform sensitivity to infused agents makes direct prediction of threshold shifts difficult, the technique allows for comparison of infusion protocols. A fixed flow rate of 16 nl/min (1 μl/hr) was used as this has been shown to have limited impact on cochlear function (Chen et al., 2006). A higher flow rate at 32nl/min was also examined. For all experiments, long infusion tubing connected to a syringe pump was used with different fluids separated by ~10 nl air bubbles to avoid within-tube diffusion. Initial infusion of AP confirmed no surgical impact to auditory function, with subsequent SAL and then AP washout. Threshold shifts were calculated by subtraction of the pre-surgery baseline measurement at each frequency, with statistical analysis of differences between surgical approaches (methods). Statistical significance of peak response and recovery when compared to baseline were also performed.

Custom Surgical Equipment

To facilitate surgical consistency and limit cochlear damage, insertion stops were created on carbide microdrills (Drill Bit City, Prospect Heights, IL) used to make the cochleostomy and canalostomy openings. Polyimide coated fused silica capillaries of 353 μm OD, 201 μm ID (Polymicro Technologies, Phoenix, AZ) were cut into 2 mm lengths using a wafer saw, and cleaned with isopropyl alcohol. For each drill bit, a cut capillary section was manually positioned over the drill shank under a microscope using forceps. The insertion depth was controlled by careful length measurement of the exposed drill bit tip against stacks of shim stock of known thicknesses (Precision Brand, Downers Grove, IL). The capillary section was glued in place with cyanacrolyate adhesive (Loctite 4206) and dental cement (3M ESPE Durelon). Insertion depths of 102, 127, 153, and 178 μm were created on microdrills of 175 μm and 100 μm diameters.

The use of silicone insertion stops on the infusion tubing has been reported in the literature to limit the depth of penetration (Kingma, et al., 1992; Chen, et al., 2006; Johnson et al., 2007). For the present study, more effective seals were produced by direct bonding to the polyimide cannulae without insertion stops, so the stops were not used. To mitigate risks associated with uncontrolled penetration into scala tympani, a micromanipulator was used to insert the tubing into the cochleostomy hole with a target insertion depth of 150 μm.

Animals and Surgical Procedures

A total of 28 young adult (age 2-4 months) CBA/CaJ mice, bred and raised in-house, were divided into two groups: CO and C+C. 16 animals were used for the 16nl/min flow rate and 12 animals for the 32nl/min flow rate. All animal experiments were approved by the University of Rochester Committee on Animal Resources, and were performed using accepted veterinary standards.

For the CO approach, animals were deeply anesthetized with a mixture of ketamine/xylazine (120 and 10 mg/kg body weight, respectively, intraperitoneal injection (IP)), and the left ventral surface of the neck was shaved and cleaned. For animals also receiving the canalostomy (C+C approach), the left post-auricular region was shaved and cleaned. The animal was positioned on a heated operative plane on their back under aseptic conditions. Surgery was performed on the left (ipsilateral) ear. Following the procedures initially developed by Jero and colleagues (2001) and modified by Chen and co-workers (2006), the tympanic bulla was exposed by a ventral approach. Under an operating microscope, an incision was made longitudinally along

the ventral surface of the neck, extending from the angle of the mandible to the level of the clavicle. The submandibular gland was retracted laterally to expose the digastric muscle which was cut with an electrocautery to expose the bony tympanic bulla and the stapedial artery. The stapedial artery was carefully lifted from the surface of the bulla and cauterized at the entrance to the bulla with care taken to minimize cochlear heating. The surrounding tissue was removed to expose the inferior-medial aspect of the bulla which was carefully cleaned and dried. A cochleostomy was drilled by hand at a location approximately 300 μm below the stapedial artery stump using 175 μm diameter carbide micro drills modified to include insertion stops. Sequentially longer insertion depth 175 μm bits were used (153 and 178 μm), with cochlear entry determined by a subtle change in mechanical resistance.

Using a micromanipulator (MM3-3, World Precision Instruments, Sarasota, FL), a fine metal probe and adhesive (3M Repositionable 75 spray adhesive) loosely attaching the polyimide infusion tubing to the probe, the infusion tubing was inserted into the cochleostomy. Medical grade adhesive (Loctite 4206, Rocky Hill, CT) was used to temporarily secure the infusion tubing to the bulla opening, with subsequent application of dental cement (3M ESPE Duralon, St. Paul, MN) providing a more permanent and robust bond, sealing the cannula to cochleostomy site. Pilot experiments with infusion of dye confirmed no leakage around the cochleostomy site with this approach. The surgery site was loosely sutured closed for this acute experiment to provide strain relief for the infusion tubing.

For animals also receiving the canalostomy (C+C approach), following the cochleostomy procedure described above the animal was positioned on a heated operative plane on their stomach under aseptic conditions. Under an operating microscope, an incision was made behind the left pinna and the muscles separated to expose the posterior semicircular canal. A hole was drilled in the posterior semicircular canal with a 100 μm diameter drill bit modified with an insertion stop. Sequentially longer bits were used (102 and 127 μm), with canal entry determined by a subtle change in mechanical resistance. The canalostomy was loosely covered with muscle for the duration of the experiment.

During infusions, mice remained immobilized by anesthesia as described above, with supplementary doses (1/3 of the initial dose) administered as needed to maintain the proper levels of general anesthesia. Parameters such as foot or tail pinch, palpebral reflex and respiratory rate were monitored to indicate the need for supplemental doses.

Drug Infusion System and Solutions

AP and SAL solutions were delivered to the basal turn of scala tympani through a 30-40 cm length of U S Pharmacopoeia Class VI polyimide tubing (044-I; ID 110 μm; OD, 139 μm; Microlumen, Tampa, FL). The infusion tubing was connected to a 25 μl Hamilton syringe (1702 RNR 22S/2”) using a PEEK nanotight fitting (Upchurch Scientific, Oak Harbor, WA). The syringe was mounted in a syringe pump (UMP2, World Precision Instruments, Sarasota, FL) allowing precise control of infusion rates. A schematic illustration of the infusion setup is shown in Figure 1.

The volume of the infusion tubing was sufficient to contain the initial AP and subsequent SAL solutions. The syringe was carefully filled with AP, with all trapped air removed via repeated rapid aspiration and ejection. The infusion tubing was then connected and filled via syringe ejection. Defined volumes of solution and air were then pre-loaded into the infusion tubing through aspiration of AP, air, and SAL. The final volumes were as depicted in Figure 1, with the initial 1000 nl of AP providing ample volume for post-surgery auditory assessment prior to delivery of SAL. The subsequent AP provided washout of SAL, and confirmation that auditory thresholds returned to baseline conditions. The inclusion of ~10 nl air bubbles between solutions avoided within-tube diffusion, and in the present study had no impact on auditory

measures. The tubing tip was left immersed in AP until being attached to the micromanipulator immediately prior to drilling the cochleostomy hole. At this time, infusion at 16 nl/min was started to ensure that evaporation at the tubing tip did not incorporate an air bubble of variable and uncontrolled size. Infusion continued during insertion of the cannula tube and the gluing process. For flow rate experiments, the flow rate was increased from 16 to 32 nl/min following post-surgery auditory assessment. While the exact amount of *initial* AP injected was variable, the point of SAL delivery was known via the dispensed volume.

The control solution and base for the SAL solution was AP with a composition (in mM) of: NaCl, 120; KCl, 3.5; CaCl2, 1.5; glucose, 5.5; and HEPES buffer, 20 (Chen et al., 2006). The pH was adjusted to 7.5 with NaOH and the solution filter sterilized and stored for later use. 10 mM sodium salicylate (JT Baker, Phillipsburg, PA) solutions were mixed on the day of experiment using the prepared AP solution.

Auditory Function Assessment

Auditory function was assessed via automated DPOAE threshold measurements at F2 frequencies 8.94, 13.45, 17.89, 24.60, 35.78, and 49.19 kHz. Measurements were performed prior to surgery, immediately following surgery, and approximately every 12 minutes during infusion. Mice were anesthetized as described above with supplementary doses administered as needed. Prior to recordings, the ear canals and ear drums were inspected for signs of obstruction or infection, and only those animals with clear outer and middle ears were used. While under anesthesia, body temperature was maintained at 38°C with a heating pad. Recording sessions were completed in a soundproof acoustic chamber (IAC) with measurements performed on both ears. Contralateral ear DPOAE thresholds provided a control for non-infusion related auditory threshold shifts.

Tucker Davis hardware (TDT; Alachua, FL) was controlled via ActiveX from a custom Matlab r13 (Mathworks; Natick, MA) graphical user interface. Sound stimuli were generated and signals acquired using Tucker Davis RP2.1 processors running at a sample rate of 195312.5 Hz. All signals were played through two electrostatic speakers (TDT EC1) connected by 4 cm tubes to a probe containing an ER10B+ microphone (Etymotic; Elk Grove Village, IL); the entire speaker and probe assembly were mounted in an adjustable vibration-isolating frame on a micromanipulator arm. All recorded signals were loaded into Matlab r13 for analysis. Waveforms from each individual presentation were windowed using a Hamming window and high-resolution 390625-point FFTs (2x sample rate) were calculated. The resulting FFTs had a bin size of 0.5 Hz allowing for accurate measurement of signal level as a function of frequency. Frequency-domain averaging was used to minimize artifacts; FFTs for multiple repetitions of the same stimulus were averaged together before subsequent analysis. The probe microphone was calibrated relative to a ¼” B&K microphone (Type 4938, Bruel & Kjaer; Naerum, Denmark) using a 0.1 cc coupler (simulating the mouse ear canal).

DPOAE amplitudes were measured in the following manner: two primaries (F1 and F2) were generated at 65 and 50 dB SPL, respectively. The ratio of the two frequencies was 1.25. Waveforms of the output of the ER10B+ probe microphone were captured on a TDT RP2.1. FFTs for each presentation were averaged together and the signal level at five frequencies was sampled: F1, F2, DP (2F1-F2), and two noise bins above and below the DP frequency. Following FFT sampling, dBV was converted to SPL based on the ER10B+ microphone calibration.

DPOAE Thresholds were defined as the F1 level required to produce a DP of 0 dB SPL (+/- 1 dB). We developed an automatic threshold search algorithm implemented in Matlab r13 using TDT hardware and the Etymotic ER10B+ probe microphone. The measurement of DP threshold was interleaved with DP amplitude measures described above and began with two

primaries as above at 65 and 50 dB SPL. Based on the distance of the DP from its target level of 0 dB SPL (distance henceforth: DP error), F1 and F2 level on the subsequent trial was incremented (or decremented) by 0.6 of this distance; e.g., if the DP was at 10 dB SPL, F1 F2 were decremented by 6 dB. F2 level was always F1–15 dB. The 0.6 “approach factor” was determined empirically to be an optimal rate of approach combining rapid acquisition of threshold and minimal oscillation around the target. Due to extremely steep DP I/O functions around 0 dB and the resulting overshoot of DP amplitude, occasionally on successive trials the DP amplitude may oscillate around 0 dB. In each case of oscillation, defined as three trials in which the sign of the DP error changes each trial, the approach factor was automatically made smaller by a factor of 1.5. This iterative procedure allowed rapid convergence on DP threshold while preventing overshoot. Once the DP was measured to be within 1 dB of 0 dB SPL, the identical F1 level was presented again for confirmation. Identification of thresholds requires two successive trials of F1 F2 levels that evoked a 0 dB SPL DP amplitude.

Modeling and Simulated Concentration Gradients

All simulations were performed with FluidSim V1.6i (Salt, 2005) using the mouse template and perfusion/flow option. Parameter values within the model were: duration (65 min), output interval (20 sec), molecular weight of solute (137 g/mol), inflow chamber (scala tympani), inflow location to approximate the cochleostomy site (1.3 mm), infusion rate (16 nl/min or 32nl/min), interscala and scala-to-blood communication half-time (30 min). All other parameters remained at their default values. Selection of the fluidic exit within the model allowed simulation of the two delivery approaches. For the CO approach, the exit was placed in the basal turn of scala tympani (0.1 mm) to approximate the location of the cochlear aqueduct. In the C+C simulation, the exit was placed at the basal turn of scala vestibuli (0.1 mm) to approximate the vestibular system (not represented in the FluidSim model). Since the program allows for only a single fluidic exit, flow through the cochlear aqueduct was not modeled in the C+C simulation.

Model parameters were chosen to closely approximate the *in vivo* experiments, with interscala communication modeled as a constant cross section with a half-time based on published measurements in guinea pig with trimethylphenylammonium (Salt et al., 1991). Relative solute concentration was set arbitrarily at 1000, with results normalized to this starting concentration for all simulations. Predicted solute concentration versus position in scala tympani was extracted at the end of the experiment and compared to *in vivo* DPOAE threshold shifts at the same time point for both surgical approaches (1000 nl SAL infusion). While non-linear sensitivity effects may make direct correlation of threshold shift to concentration difficult, this approach allows for investigation of general trends and comparison of surgical approaches. A physiological place-frequency map of the mouse cochlea (Müller et al., 2005) allowed correlation of DPOAE responses with cochleotopic position. The characteristic frequency was related to the DPOAE F2 frequency, with a scala tympani length of 4.55 mm utilized (Thorne et al., 1999).

The impact of flow rate on velocity profiles and fluid jet mixing was investigated using an idealized, linear cochlear model of scala tympani and numeric modeling using a commercial finite element program (COMSOL Multiphysics). In this two step simulation process, the fluid velocity and pressure field were first calculated via a steady form of the momentum equation. Subsequently, the transport of a soluble dye with prescribed concentration at the inlet was modeled with a time-dependent solution of diffusion and convection using the simulated velocity field. The diffusion constant was set to zero in order to isolate convective transport and allow visualization of flow and mixing mediated spread. The inlet velocity was set as 28μm/sec or 56μm/sec, corresponding to flow rates of 16nl/min and 32nl/min respectively. The outflow was maintained at ambient pressure and the no slip condition prescribed to all

walls. The long tube modeling the cochlea was closed at its distal end (apex) and was not porous. The geometry was composed of ~80,000 tetrahedral elements.

The model assumed a circular cross-section of variable diameter with the cochlear aqueduct located at 0.1mm from the basal end. Diameters were extracted from scala tympani cross-sectional areas (Thorne et al, 1999); diameters included in the model were 0.11 mm at the base, 0.48 mm at 0.7 mm from the base, 0.32 mm at 1.4 mm to 3.9 mm from the base, and 0.23 mm at 4.1 mm to 4.5mm from the base. Both velocity profiles and steady-state concentrations were evaluated at 16 nl/min and 32 nl/min flow rates, with apical spread qualitatively compared.

Statistical Analyses

DPOAE threshold shift data were collected from each experiment with three consecutive data points averaged for each animal approximating the half-way point of salicylate infusion, end of salicylate infusion, and washout. Two-way analysis of variance (ANOVA) with repeated measures and exclusion of pre-SAL threshold data allowed comparison between surgical approaches and flow rates (Prism, GraphPad, La Jolla, CA). Responses are graphically shown as a mean ± SEM for all animals receiving each surgical approach. Bonferroni post-hoc analysis for multiple comparisons was used to evaluate threshold shifts in response to SAL infusion for each frequency tested. These comparisons used the true peak for each animal rather than the three point average.

Results

The theoretical and simulated flow conditions for the CO and C+C infusion experiments are represented in Figure 2. Frequency dependent DPOAE thresholds were measured during infusions with resulting threshold shifts compared to predicted salicylate concentrations along the length of scala tympani.

Frequency Dependent DPOAE Threshold Shifts with Salicylate

Salicylate has been shown to act as a competitive antagonist at the anion-binding site of prestin, resulting in an inhibition of outer hair cell electromotility (Oliver et al., 2001). This inhibition decreases the magnitude of otoacoustic emissions (Brownell et al., 1990), and can be measured as a reversible elevation of DPOAE thresholds. This has been previously demonstrated with intracochlear delivery of salicylate in the mouse where threshold elevations and subsequent washout and recovery were observed (Chen et al., 2006). In the present study, DPOAE thresholds were measured during intracochlear infusion of SAL for both surgical approaches. Average threshold shifts and statistical significance of peak response compared to baseline across frequencies for each surgical approach are presented in Figure 3. Both surgical approaches allow direct, intracochlear delivery of compounds without acute impact to auditory function as demonstrated by stable thresholds during the initial AP infusion and subsequent threshold recovery during the washout phase. Greater shifts at high frequencies are consistent with higher salicylate concentrations in the basal turn of the cochlea; near the point of infusion. The CO approach provided statistically significant threshold shifts from baseline for 17.9, 24.6, 35.8 and 49.2 kHz, while the C+C approach provided statistically significant threshold shifts at all frequencies tested, suggesting enhanced access to apical cochlear structures.

Cochleostomy-plus-Canalostomy Reduces Concentration Gradients

Comparison of the two surgical approaches is best accomplished by examination of the time course of DPOAE threshold shifts for each measured frequency as shown in Figure 4. The point of infusion is presumed to be close to the 35.8 kHz cochlear location based on the similarity of threshold shifts for the two surgical approaches at this frequency. Statistically significant differences between methods are observed at 13.5, 17.9, 24.6, and 49.2 kHz, with

the most significant differences occurring for more apical frequencies, consistent with the hypothesized pressure driven flow path.

Comparison of Simulated Concentration Gradients to Auditory Response

DPOAE threshold shifts were compared against simulated concentration gradients within scala tympani for both surgical approaches as shown in Figure 5. The CO simulation and measured response were qualitatively similar, with the model exhibiting the expected diffusion mediated concentration dependence. However, the slope of the measured threshold shift versus distance was greater than that observed for the simulated concentration. Simulation of the C+C infusion resulted in higher predicted apical concentrations; predictions which did not match the measured physiological response. These simulations also under-estimate concentrations more basal than the infusion point since pressure driven outflow through the cochlear aqueduct could not be modeled simultaneously with the canalostomy outflow. The most basal C+C concentrations were lower than the CO concentrations, while the high frequency DPOAE threshold shifts were greatest in the C+C case.

Higher Flow Rates Enhance Low Frequency Threshold Shifts

DPOAE threshold shifts were compared across frequency for both surgical approaches using two flow rates; 16 nl/min and 32 nl/min. The higher flow rate caused no acute impact to auditory function as demonstrated by stable thresholds during the initial AP infusion and subsequent threshold recovery during the washout phase. The C+C infusions exhibited statistically similar thresholds shifts for both flow rates (data not shown). For the CO approach, statistically significant shifts from baseline were observed for 17.9, 24.6, 35.8 and 49.2 kHz for the 16 nl/min flow rate, while increasing the flow rate to 32 nl/min enabled statistically significant shifts to be observed down to 13.5 kHz. This suggest increasing flow rate results in higher concentrations at more apical regions of the cochlea.

The time course of threshold shift for the CO infusions are shown in Figure 6. There was a statistically significant difference between methods at 13.5 and 17.9kHz with enhanced response for the higher flow rate, suggesting flow rate may be an important variable in optimization of intracochlear drug delivery paradigms.

FluidSim simulations were performed for the CO infusion at both 16 and 32 nl/min infusion rates, with a higher concentration predicted for the higher flow rate as shown in Figure 7a. Simulations of the effect of clearance rates are shown in Figure 7b demonstrating the anticipated strong dependence of resulting concentration on clearance rate. To determine if the higher flow rate results in enhanced fluidic mixing and apical spread due to fluid jet impingement on the scala tympani wall, a computational fluid dynamics simulation was performed examining velocity profiles and resulting steady state concentrations in the absence of diffusion forces. The results of Figure 8 demonstrate similar concentration profiles and extension toward the apex for both flow rates. Fluid velocity profiles were similarly independent of flow rate. These results, coupled with the cochlear simulations of Figure 7 suggest clearance is the primary mechanism impacting flow rate enhancements.

Discussion

The new findings support the hypothesis that a fluidic exit in the posterior semicircular canal enhances access to apical structures as compared to a basal turn cochleostomy-only. The C+C approach provided statistically significant enhancement of DPOAE threshold shifts at 13.5, 17.9, 24.6, and 49.2 kHz as compared to the CO approach. The similarity in response at 35.8 kHz suggests the cochleostomy site is near the 35.8 kHz cochlear place, resulting in similar salicylate concentrations for both approaches, as would be expected. With the fluidic exit in

the posterior semicircular canal, the statistically significant enhancement in DPOAE threshold shift over the CO approach at 49.2 kHz (Figures 4 and 5) suggests higher concentrations for the most basal regions with the C+C method. This result could suggest pressure driven flow from scala tympani to scala vestibuli or the vestibule with the fluidic exit in the vestibular system. Alternatively, salicylate may enter endolymph from scala vestibuli or the vestibule in the basal turn, resulting in the larger threshold shifts. Further investigation will be required to determine if a pressure driven component of transport from scala tympani to scala vestibuli and / or the vestibule occurs in parallel with the reported measurements and simulations of diffusion mediated transport (Salt et al., 1991; Plontke et al., 2002; Zou et al., 2005). The larger threshold shifts at 13.5, 17.9, and 24.6 kHz suggest higher concentrations of salicylate for these more apical frequencies. These results support the hypothesis that a fluidic exit in the vestibular system will facilitate longitudinal flow from cochlear base to apex. This enhanced access to apical structures has important implications for deafness therapy research. Reduced cochlear concentration gradients are important for compounds with a narrow therapeutic dose range, and access to apical structures is critical for therapies including or targeting low frequency dysfunction. These concentration gradients, while significant in the mouse, are likely to be larger in other rodents, such as gerbils or guinea pigs, higher mammals and in humans where size will limit efficacy of diffusion mediated distribution.

The simulation results provided limited additional insight into the specific delivery approaches examined herein. The simulated CO concentration profile was qualitatively similar to the frequency dependent DPOAE threshold shifts, however the auditory response dropped off more rapidly than the simulation. The physiological data are consistent with a positional dependence of salicylate ototoxicity, with apical outer hair cells exhibiting less sensitivity, resulting in lower DPOAE threshold shifts for equivalent concentrations. Systemic high doses of aspirin (salicylate) in humans have demonstrated ototoxic effects perceived as tinnitus or inducement of hearing loss. Hearing loss is generally bilateral, symmetrical, and affects all frequencies, with a predominance at high frequencies (Cazals, 2000). Studies of compound action potential (CAP) thresholds in gerbils in response to systemic injection of salicylic acid demonstrate frequency dependence with the greatest response for high frequencies (Müller et al., 2003). These examples, while systemic rather than intracochlear, support the hypothesis of non-uniform salicylate sensitivity. It is also consistent with observed differential vulnerability of OHC to aminoglycosides in organotypic cultures where basal OHC loss was significantly higher than apical OHC loss (Sha et al., 2001). This lower susceptibility of low-frequency, apical outer hair cells to salicylate ototoxicity would significantly complicate correlation of physiologic responses to the concentration profile; threshold shifts would be smaller in apical regions for equivalent concentrations.

The C+C simulated concentration profile was quite different than the DPOAE threshold shift profile. While positional salicylate ototoxicity dependence would partially account for the difference, model limitations clearly had an impact. Specifically, the limitation of a single fluidic exit resulted in zero modeled flow through the cochlear aqueduct; flow which will occur based on the relative fluidic resistances represented by the cochlear aqueduct and the flow path to the posterior semicircular canal canalostomy. Thus, the model results likely overestimate apical concentrations for this C+C approach. More advanced one dimensional models are needed which allow simulation of alternate infusion approaches, pressure driven flow, multiple fluidic exits, and clearance / transport parameters appropriate for the mouse cochlear model system. Three dimensional models are important for work in larger animals and humans where radial concentration gradients impact the spatiotemporal profile of delivered agents (Plontke et al., 2007). Future models will require inclusion of the vestibular system, and more accurate estimation of fluidic geometries and compartments, clearance rates, diffusion coefficients, interscala transport coefficients, fluidic resistance paths, and pressure gradients, before

simulations can be used to accurately predict distribution profiles for optimization of intracochlear drug delivery approaches.

Flow rate had a minimal impact on DPOAE thresholds across all frequencies tested for the C +C infusion approach. However, a doubling of flow rate to 32nl/min for the CO infusions resulted in statistically significant increases in threshold shifts for 13.5 and 17.9 kHz, suggesting increased concentration in apical regions due to the higher flow rate. This suggests either compensation for clearance resulting in higher concentrations at the infusion point and greater diffusion forces, or enhanced fluidic mixing due to fluid jet impingement on the opposite wall of scala tympani. The results of Figures 7 and 8 suggest minimal mixing from turbulence, with clearance as the primary mechanism impacting flow rate enhancements. The impact of clearance rates on concentration (Figure 7b) saturates, suggesting a similar effect will be observed with concentration enhancements with flow rate. The lack of statistically significant shifts in DPOAE thresholds for the C+C infusions at 32 nl/min is consistent with this saturation effect, since higher SAL concentrations are predicted throughout the cochlea.

Recent advances in transgenic and gene targeting technologies in mice, and the sequencing of the mouse genome, offer extraordinary opportunities to manipulate and study the effect of different genes on auditory function *in vivo*. Numerous inbred mouse strains have been identified as models of deafness and presbycusis, and the potential exists to replicate mutations found to contribute to hearing loss in humans. Understanding of inner ear drug delivery methodologies and control of resulting concentration gradients will become increasingly important for development of advanced therapies addressing the biological basis of auditory dysfunction. Access to apical structures can be enhanced through an alternate surgical approach (C+C) providing pressure driven flow through the cochlea. However, correlation of concentration gradients to physiological response is potentially complicated by non-uniform sensitivity to salicylate throughout the cochlea. Future work should involve more direct measures of drug concentration as has been done in the guinea pig with TMPA (Salt et al., 1991), but utilizing methods appropriate given the size limitations of the mouse cochlea. The study of pharmacokinetics of drug delivery in the inner ear will become increasingly important for the development of new therapeutics in animal models. Computer models of the cochlea provide opportunities to test different delivery methodologies and infusion parameters, and explore potential clearance rates and modes of interscalar exchange. Expansion of currently available models to incorporate pressure driven flow with multiple fluidic outlets will enhance their predictive capability.

Supplementary Material

Refer to Web version on PubMed Central for supplementary material.

Acknowledgments

This work supported by NIH Grants from the National Institute on Deafness and other Communication Disorders (K25-DC008291 and P30 DC05409) and the National Institute on Aging (P01 AG09524). The author's would like to thank Dr. Alec Salt, Washington University School of Medicine, for his help in determining appropriate input parameters for FluidSim; Dr. Owen Brimijoin, University of Rochester Medical Center, for developing the Matlab based DPOAE thresholding program; and Dr. Steven Day and Oyuna Myagmar, Rochester Institute of Technology, for assistance with the COMSOL Multiphysics modeling of cochlear flow.

Abbreviations

AP	artificial perilymph
CAP	compound action potential

C+C	cochleostomy-plus-canalostomy
CO	cochleostomy-only
DPOAE	distortion product otoacoustic emissions
FFT	fast Fourier transform
ID	inner diameter
IP	intraperitoneal injection
OD	outer diameter
RWM	round window membrane
SAL	10mM sodium salicylate

References

Borkholder DA. State-of-the-art mechanisms of intracochlear drug delivery. Current Opinions in Otolaryngology & Head and Neck Surgery 2008;16:472–477. 2008.

Brownell WE. Outer hair cell electromotility and otoacoustic emissions. Ear Hear 1990;11:82–92. [PubMed: 2187727]

Cazals Y. Auditory sensori-neural alternations induced by salicylate. Progress in Neurobiology 2000;62:583–631. [PubMed: 10880852]

Chen Z, Kujawa SG, McKenna MJ, Fiering JO, Mescher MJ, Borenstein JT, Leary Swan EE, Sewell WF. Inner ear drug delivery via a reciprocating perfusion system in the guinea pig. J. Controlled Release 2005;110:1–19.

Chen Z, Mikulec AA, McKenna MJ, et al. A method for intracochlear drug delivery in the mouse. J Neurosci Methods 2006;150:67–73. [PubMed: 16043228]

Jero J, Tseng CJ, Mhatre AN, Lalwani AK. A surgical approach appropriate for targeted cochlear gene therapy in the mouse. Hearing Research 2001;51:106–114. [PubMed: 11124456]

Johnson, DG.; Zhu, XX.; Frisina, RD.; Borkholder, DA. Micro-molded cannulae for intracochlear infusions in small rodents.. Proceedings of the 29th IEEE Annual Engineering in Medicine and Biology Society Conference; Lyons, France. August 23-26; 2007.

Kawamoto K, Oh SH, Kanzaki S, et al. The functional and structural outcome of inner ear gene transfer via the vestibular and cochlear fluids in mice. Mol Ther 2001;4:575–585. [PubMed: 11735342]

Kingma GG, Miller JM, Myers MW. Chronic drug infusion into the scala tympani of the guinea pig cochlea. J. Neuroscience Methods 1992;45:127–134.

Müller M, Klinke R, Arnold W, Oestreicher E. Auditory nerve fiber responses to salicylate revisited. Hearing Research 2003;183:37–43. [PubMed: 13679136]

Müller M, von Hünerbein K, Hoidis S, Smolders JWT. A physiological place-frequency map of the cochlea in the CBA/J mouse. Hearing Research 2005;202:63–73. [PubMed: 15811700]

Nakagawa T, Kim TS, Murai N, Endo T, Iguchi F, Tateya I, Yamamoto N, Naito Y, Ito J. A novel technique for inducing local inner ear damage. Hearing Research 2003;176:122–127. [PubMed: 12583887]

Oliver D, He DZZ, Klöcker N, Ludwig J, Schulte U, Waldegger S, Ruppersberg JP, Dallos P, Fakler B. Intracellular anions as the voltage sensor of prestin, the outer hair cell motor protein. Science 2001;292:2340–2343. [PubMed: 11423665]

Plontke SK, Wood AW, Salt AN. Analysis of gentamicin kinetics in fluids of the inner ear with round window administration. Otol Neurotol 2002;23:967–974. [PubMed: 12438864]

Plontke SK, Siedow N, Wegener R, Zenner HP, Salt AN. Cochlear pharmacokinetics with local inner ear drug delivery using a three-dimensional finite-element computer model. Audiol Neurootol 2007;12(1):37–48. [PubMed: 17119332]

Plontke SK, Biegner T, Kammerer B, et al. Dexamethasone concentration gradients along scala tympani after application to the round window membrane. Otology & Neurotology 2008;29:401–406. [PubMed: 18277312]

Roehm P, Hoffer M, Balaban CD. Gentamicin uptake in the chinchilla inner ear. Hear Res 2007;230:43–52. [PubMed: 17616288]

Salt, AN. Cochlear fluids simulator V 1.6i. 2005. released December 2005, http://oto2.wustl.edu/cochlea

Salt AN, Ohyama K, Thalmann R. Radial communication between the perilymphatic scalae of the cochlea. II: estimation by bolus injection of tracer into the sealed cochlea. Hearing Research 1991;56:37–43. [PubMed: 1769923]

Sha SH, Taylor R, Forge A, Schacht J. Differential vulnerability of basal and apical hair cells is based on intrinsic susceptibility to free radicals. Hearing Research 2001;155(1-2):1–8. [PubMed: 11335071]

Stöver T, Yagi M, Raphael Y. Transduction of the contralateral ear after adenovirus-mediated cochlear gene transfer. Gene Ther 2000;7:377–383. [PubMed: 10694819]

Thorne M, Salt AN, DeMott JE, Hensen MM, Henson OW Jr. Gewalt SL. Cochlear fluid space dimensions for six species derived from reconstructions of three-dimensional magnetic resonance images. Laryngoscope 1999;109:1661–1668. [PubMed: 10522939]

Zou J, Pyykko I, Bjelke B, Dastidar P, Toppila E. Communication between the perilymphatic scalae and spiral ligament visualized by in vivo MRI. Audiol Neurootol 2005;10:145–152. [PubMed: 15724085]

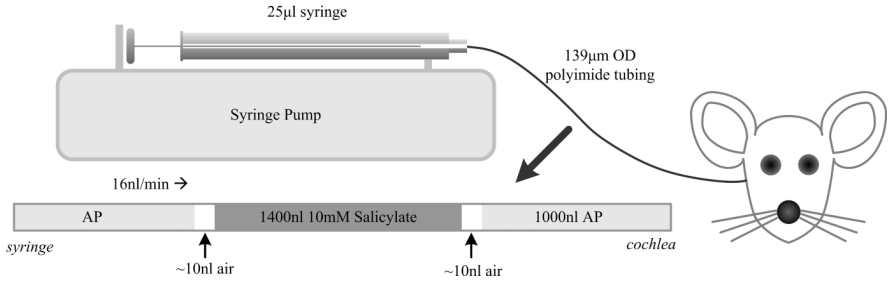

Figure 1.
Schematic illustration of the experimental infusion setup. Polyimide microtubing was preloaded with 1000 nL of AP, 1400 nL of SAL, and the washout volume of AP. Fluids were separated by a 10 nL air bubble to prevent mixing of solutions. The setup was attached to a syringe pump to precisely control infusion rate.

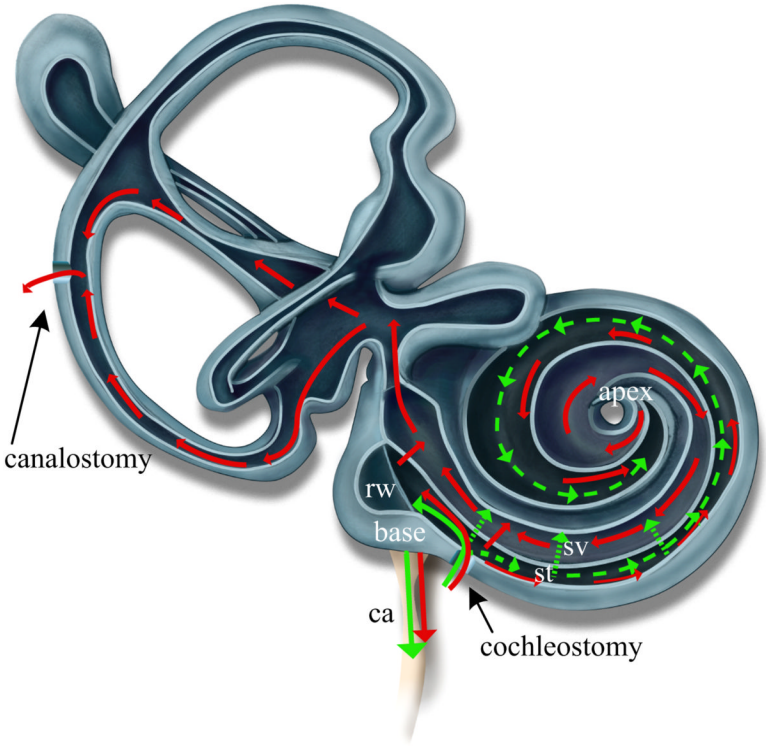

Figure 2.
Theoretical flow path within the cochlea and vestibular system for two surgical approaches. Pressure driven flow is depicted with solid lines while dotted lines represent diffusion mechanisms. Cochleostomy-only (Green) results in pressure driven outflow through the cochlear aqueduct (ca) and diffusion driven transport from base to apex and between scala. Cochleostomy-plus-canalostomy (Red) results in pressure driven flow through the cochlear aqueduct, between scala, and from base to apex in scala tympani (st), through the helicotrema, from apex to base in scala vestibuli (sv), and then through the vestibular system. Diffusion mechanisms (not shown) are similar to the CO case. Modeling of these infusion approaches with FluidSim was constrained to a single fluidic exit placed at either the ca or the base of sv..

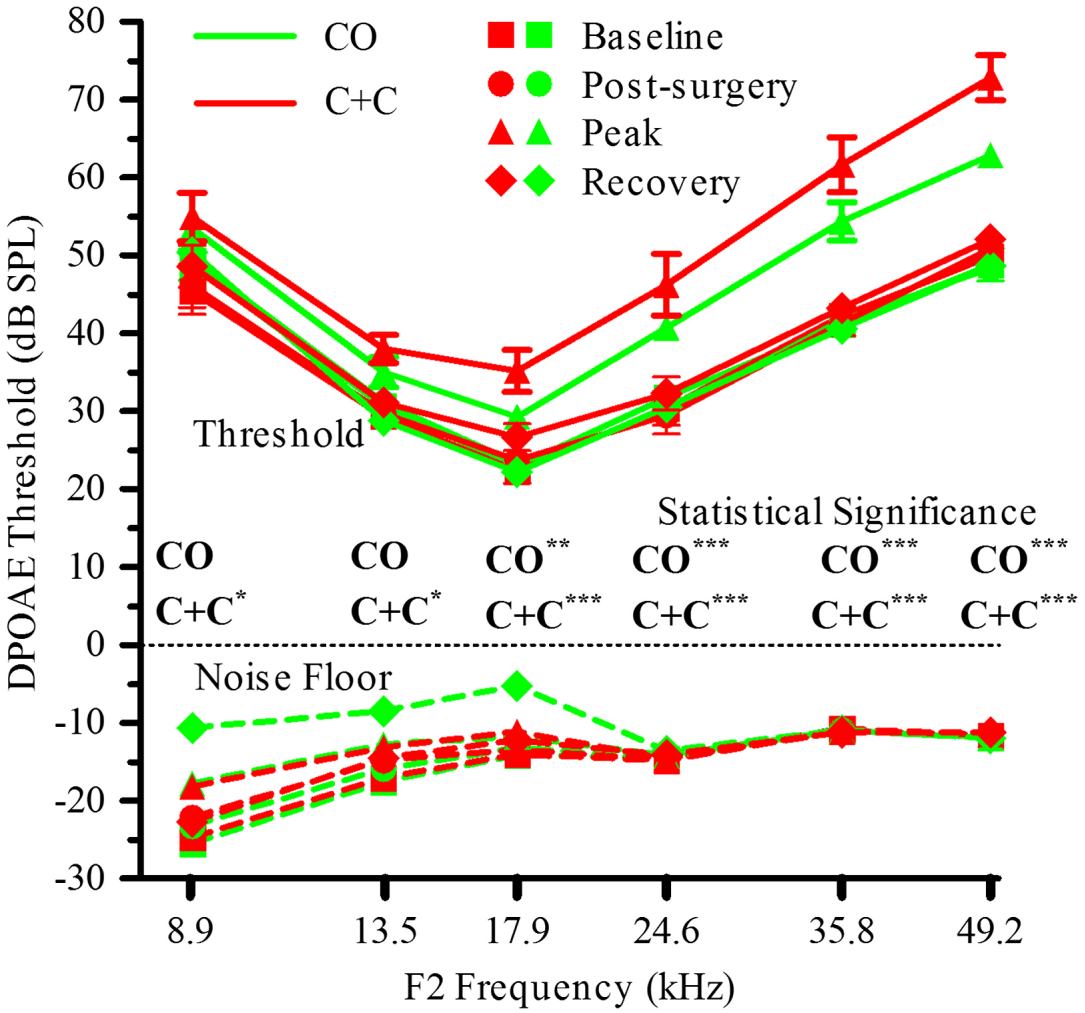

Figure 3.

Frequency dependent DPOAE threshold shifts with infusion (16 nl/min) of 1000 nl AP, 1400 nl 10 mM SAL, and ~2000 nl AP. Surgery and infusion of AP resulted in statistically insignificant shifts in DPOAE thresholds while frequency dependent shifts were observed in response to SAL. Statistical comparison of peak threshold shifts to baseline for each frequency and each surgical approach are shown on the figure (* $p<0.05$, ** $p<0.01$, *** $p<0.001$). Washout and return of thresholds to baseline values (differences statistically insignificant) suggests no acute damage to auditory function with either surgical approach. Greater shifts at high frequencies are consistent with basal turn infusion. Data are plotted as mean ± SEM (n=8 animals for each approach).

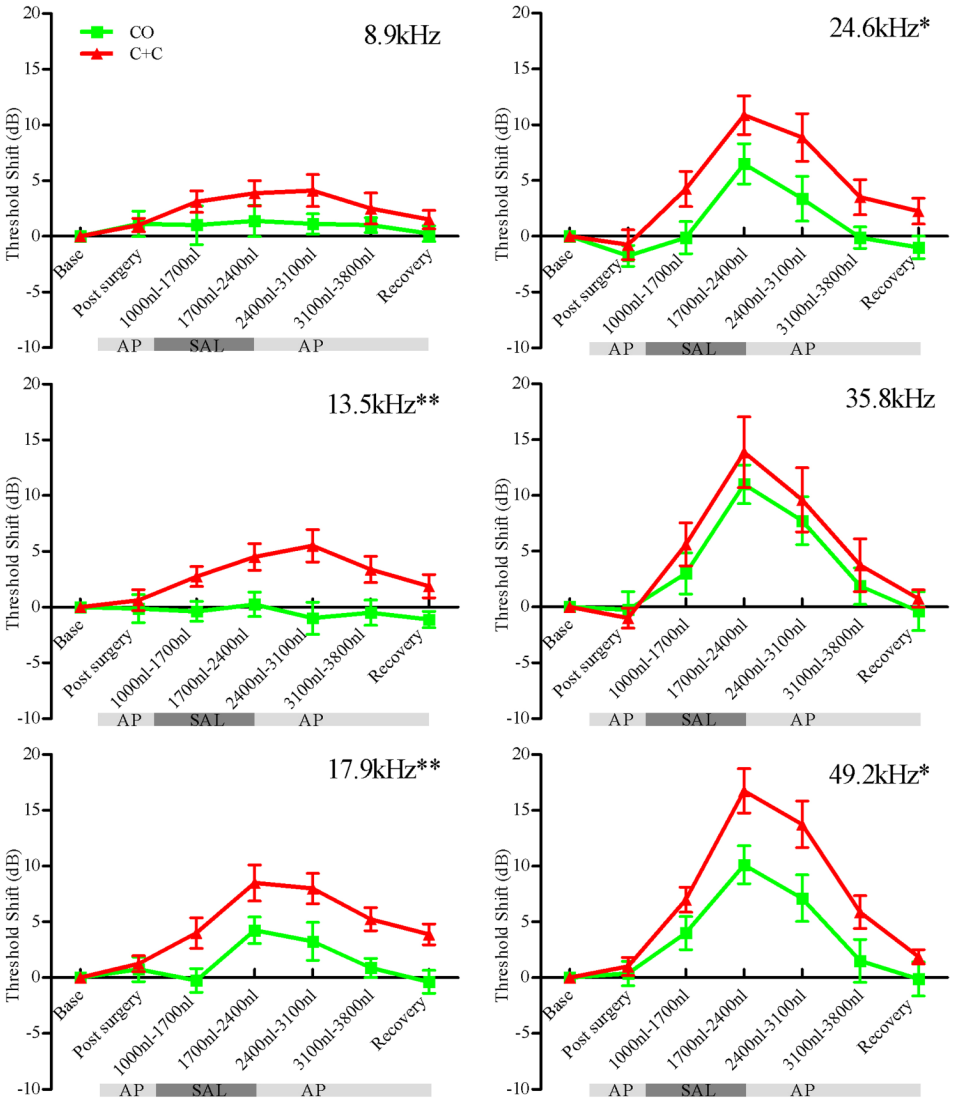

Figure 4.

DPOAE threshold shifts versus infused volumes for F2 frequencies 8.9, 13.5, 17.9, 24.6, 35.8 and 49.2 kHz. Green traces are for the CO approach while red traces are for the C+C approach. Statistically significant differences between the methods are observed for 13.5, 17.9, 24.6, and 49.2 kHz demonstrating improved access to apical structures with the C+C approach. Note that the point of infusion is presumed tonotopically close to 35.8 kHz based on similar responses at this frequency. Asterisks on figure indicate statistically significant main effects between methods (* $p<0.05$, ** $p<0.01$). Data are plotted as mean ± SEM (n=8 animals for each approach).

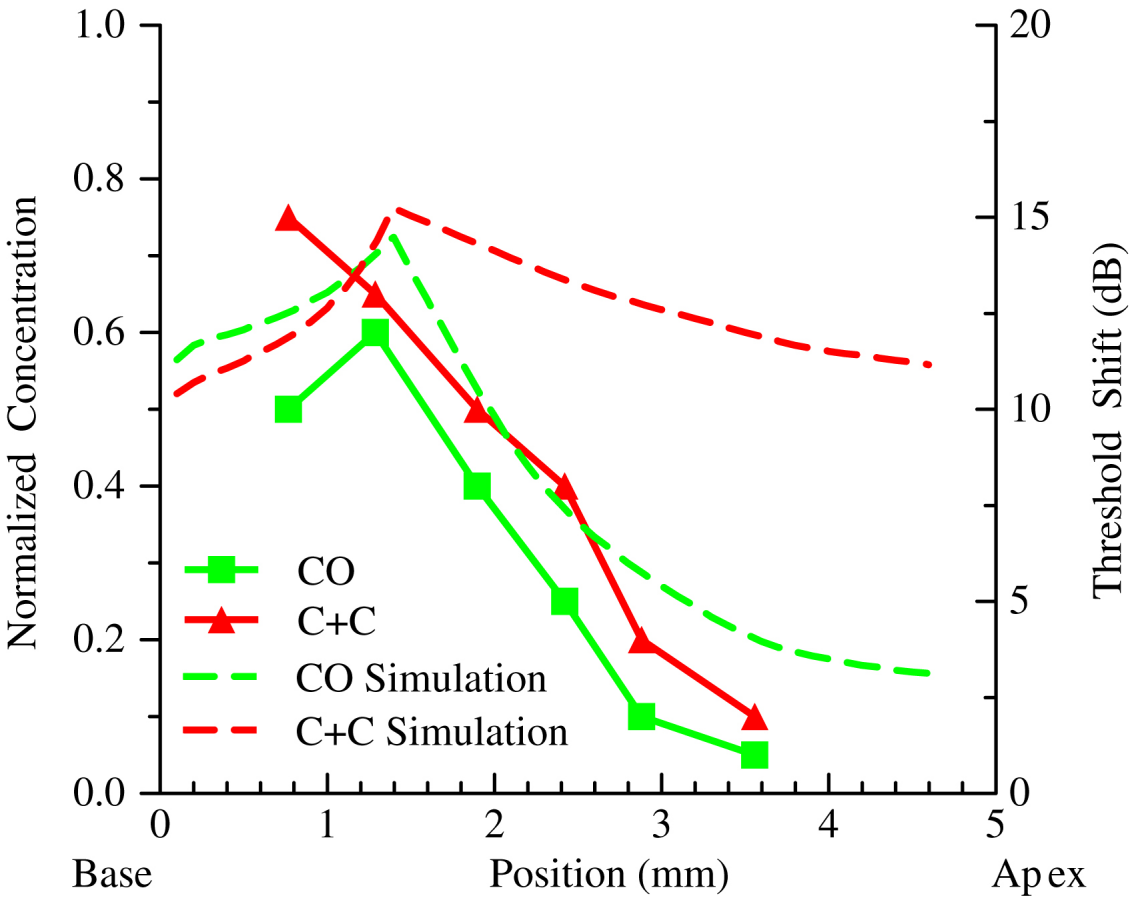

Figure 5.
Comparison of simulated concentration gradients to measured DPOAE threshold shifts. Simulated infusion is at 1.3mm. Dotted lines represent normalized drug concentrations in scala tympani following 65 minutes of simulated infusion at 16 nl/min. Data points with solid lines represent *in vivo* threshold shifts following infusion of 1000nl of SAL. The scale for threshold shift was adjusted to facilitate comparison of trends in threshold and concentration data, and does not suggest a direct correlation between the datasets. The CO data sets are qualitatively similar while the C+C threshold shifts fail to follow the shape of the predicted concentration gradient.

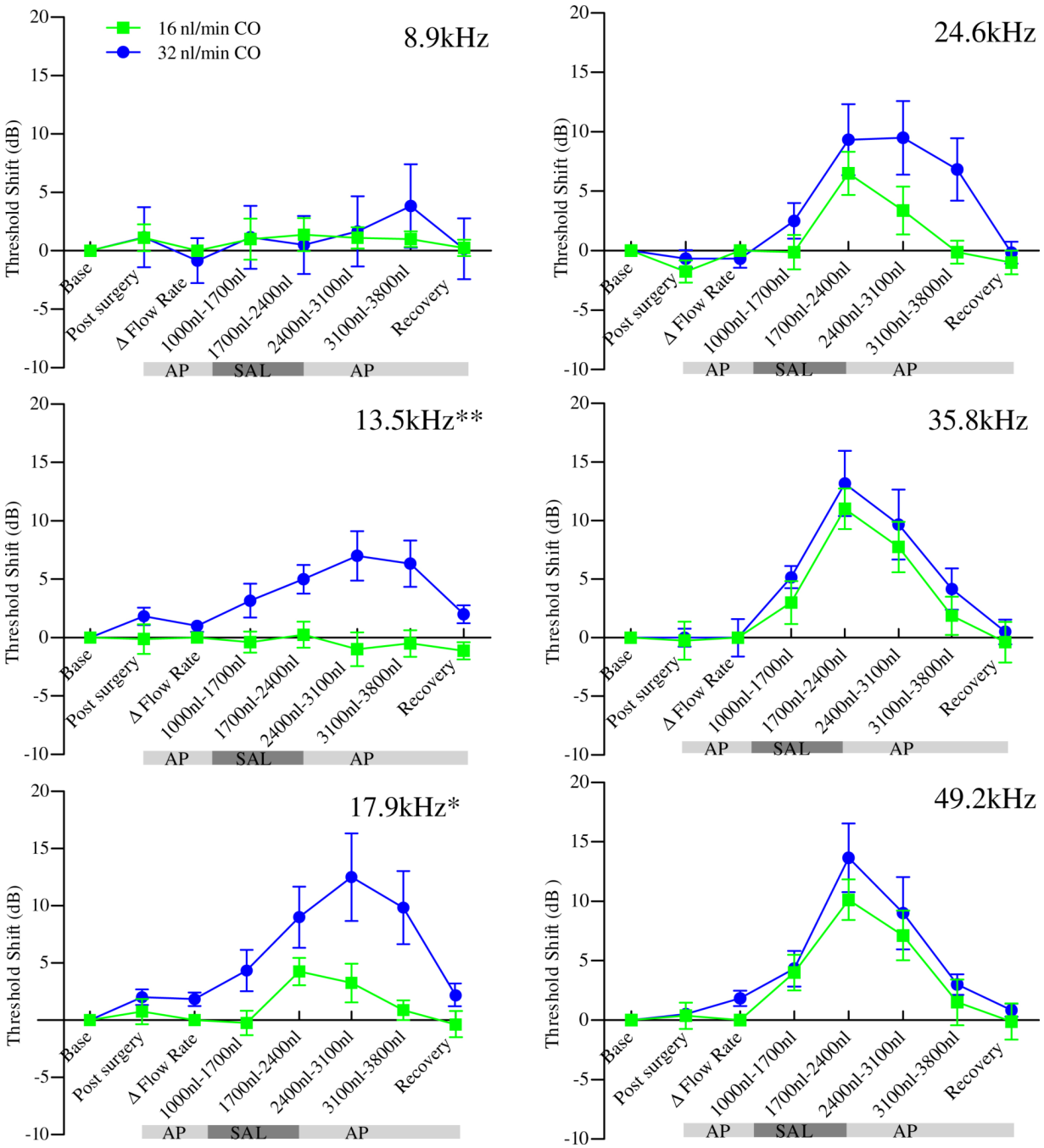

Figure 6.

DPOAE threshold shifts versus infused volumes for F2 frequencies 8.9, 13.5, 17.9, 24.6, 35.8 and 49.2 kHz. Flow rates of 16 nl / min (green) and 32 nl/min (blue) were examined for the CO approach. Δ Flow Rate indicates point at which flow was changed from 16 nl/min to 32 nl/min for the higher flow rate experiments. Statistical comparison of peak thresholds to baseline for each frequency: 16nl/min [17.9**, 24.6***, 35.8***, 49.2***], and 32nl/min [13.5**, 17.9***, 24.6***, 35.8***, 49.2***] (* p<0.05, **p<0.01, ***p<0.001). Statistically significant differences between the methods are observed for 13.5 and 17.9 kHz demonstrating higher apical concentrations with the higher flow rate. Asterisks on figure indicate statistically

significant main effects between methods (* $p<0.05$, ** $p<0.01$). Data are plotted as mean ± SEM (n=8 animals for 16nl/min and n=6 animals for 32nl/min).

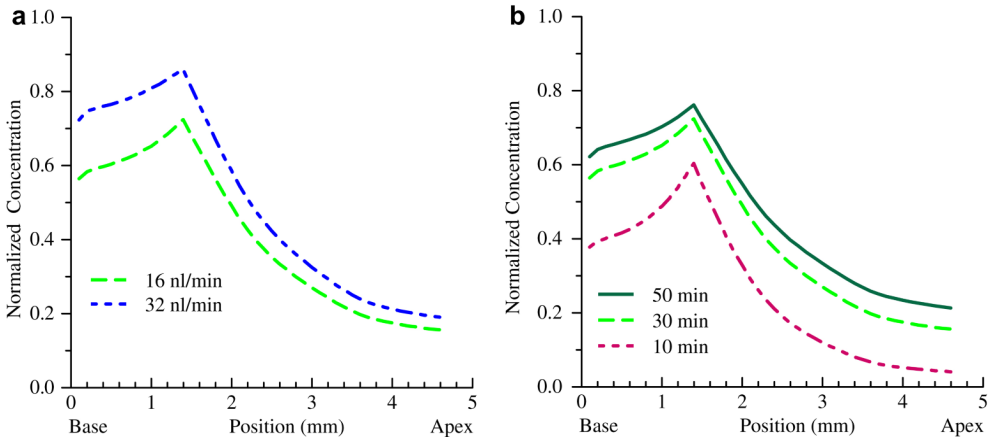

Figure 7.

Simulated concentration gradients for the CO infusion at different flow rates and clearance rates. (a) Doubling the flow rate to 32nl / min (blue) results in a predicted increase in concentration consistent with the physiological experiments. (b) Clearance rates have a significant impact on predicted concentrations as shown by the interscala and scala-to-blood communication half-times of 10, 30 and 50 minutes.

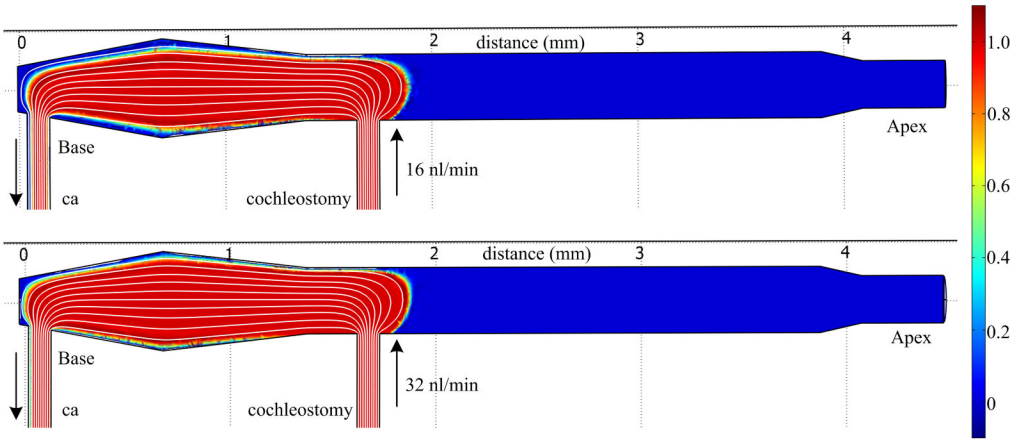

Figure 8.

Computation Fluid Dynamics (CFD) analysis of flow in an idealized, linear cochlear model of scala tympani for the CO infusion case for 16 nl/min and 32 nl/min flow rates. Diffusion forces are set to zero to isolate convective transport and allow visualization of flow and mixing mediated spread. Flow is from the cochleostomy to the cochlear aqueduct (ca). (a) The fluid velocity streamlines from the fluid jet, and resulting steady state concentrations (false color) are similar for both flow rates, suggesting the fluid dynamics have minimal impact on distribution in the cochlea. (b) Time evolution of the concentration profile for the 16nl/min flow rate (supplementary information online only).